Langmuir
Article
pubs.acs.org/Langmuir

Destruction and Solubilization of Supported Phospholipid Bilayers on Silica by the Biosurfactant Surfactin

Hsin-Hui Shen,*[,†] Robert K. Thomas,[†] Jeffrey Penfold,[‡] and Giovanna Fragneto[§]

[†]*Physical and Theoretical Chemistry Laboratory, South Parks Road, Oxford, OX1 3QZ, U.K.,* [‡]*ISIS, STFC, Chilton, Didcot, Oxfordshire, U.K., and* [§]*ILL, 6, rue Jules Horowitz, BP 156-38042 Grenoble Cedex 9, France*

Received November 5, 2009. Revised Manuscript Received January 6, 2010

The lipopeptide surfactin from *Bacillus subtilis* strains exhibits strong surface and biological activity, the latter probably because of its interaction with biological membranes. We have investigated the interaction of aqueous solutions of surfactin with supported bilayers of diphosphatidylcholine (DPPC) on silica using neutron reflectometry. We have also used small-angle neutron scattering (SANS) to study the solubilized aggregates formed as a result of the destruction of the supported membrane by surfactin. Although surfactin on its own does not attach to the silica supporting surface, it is taken up from solution by the membrane, confirming that there is an attractive interaction between DPPC and surfactin. The surfactin concentration in the layer can reach up to about 20 mol % relative to DPPC. The membrane is stable provided that the surfactin concentration is below its critical micelle concentration (cmc, 5×10^{-5} M). Above the cmc, however, the membrane is solubilized and removed from the surface, though not always completely, over a period of hours. There are signs that there is an induction period while the surfactin concentration builds up in the membrane. This would be consistent with the need for a threshold concentration of surfactin in the bilayer. The presence of a surfactin correlation peak in the SANS showed that in the bulk solution, at the same concentrations as used for the deposition, surfactin forms aggregates that must be localized in the DPPC multilamellar vesicles at a separation of about 160 Å. The structure could be fitted with an approximate model where the surfactin has an aggregation number of 50 ± 10 with a radius of about 27 Å. Given the very small water thicknesses in the DPPC lamellar aggregates, the surfactin must exist as aggregates in the phospholipid bilayer, and these structures are responsible for solubilizing the DPPC.

Introduction

In two earlier papers we have used neutron reflectometry to study the nature of the adsorbed layer of the biosurfactant, surfactin, at different types of surface[1] and to determine its location and concentration in a supported mixed bilayer of surfactin with dipalmitoylphosphatidylcholine (DPPC).[2] Surfactin is a water-soluble, highly surface-active heptapeptide (four leucines, valine, and one each of glutamic and aspartic acids) closed by a lactone group of a β-fatty acid of chain length about 14 carbons (see Supporting Information). Its structure at the air/water and at the hydrophobic/water interfaces was found to be remarkably compact, indicating that the fatty acid chain folds back toward the hydrophobic leucines in the peptide ring. The two acid groups evidently make the molecule highly amphiphilic, and this enables it to interact strongly with membranes, giving it a number of biological activities, for example, antiviral,[3] antimycoplasmic,[4,5] antibacterial,[6] and hemolytic.[7] Our earlier study of surfactin/DPPC supported bilayers focused on the formation of mixed supported bilayers; i.e., a quasi-equilibrium mixture of the two components was deposited on the support. The results showed that surfactin can be incorporated into the supported bilayer up to mole fractions of around 0.2, that the effectiveness of the deposition of the mixed layer falls with increasing fraction of surfactin in the bilayer, and that the surfactin is located in the outer leaflet of the bilayer. This is consistent with an attractive interaction between surfactin and bilayer, which brings about the mixing, and repulsion between the negatively charged surfactin and the negatively charged silica, which forms the supporting surface. We also found that the mixed bilayer would not form when the surfactin concentration was above its critical micelle concentration (cmc, 5×10^{-6} M). This suggests that the surfactin can also solubilize phospholipids, and this must also be a factor in determining its biological activity. These experiments gave no information on how surfactin is incorporated into an initially pure phospholipid bilayer nor how solubilization of the phospholipid might occur. In the present paper we explore the solubilization process in two ways. First, we have used neutron reflectometry to study the stages of removal of a pure DPPC supported bilayer by surfactin in the bulk solution. Second, we have used neutron small-angle scattering (SANS) to determine the nature of the solution aggregates formed under the same conditions that solubilization of the supported phospholipid membrane takes place.

Other studies have been made of the interaction of surfactin with biological membranes, but the molecular mechanism of the action is not understood. Several suggestions have been made,[8−11] and it is clear that it must involve some kind of insertion of the

*To whom correspondence should be addressed: e-mail hsin-hui.shen@csiro.au.

(1) Shen, H.-H.; Thomas, R. K.; Chen, C.-Y.; Darton, R. C.; Baker, S. C.; Penfold, J. *Langmuir* **2009**, *25* (7), 4211−4218.
(2) Shen, H. H.; Thomas, R. K.; Tayler, P. *Langmuir* **2010**, *26* (1), 320−327.
(3) Vollenbroich, D.; Ozel, M.; Vater, J.; Kamp, R. M.; Pauli, G. *Biologicals* **1997**, *25* (3), 289−297.
(4) Nissen, E.; Vater, J.; Pauli, G.; Vollenbroich, D. *In Vitro Cell Dev. Biol.: Anim.* **1997**, *33* (6), 414−415.
(5) Vollenbroich, D.; Pauli, G.; Ozel, M.; Vater, J. *Appl. Environ. Microbiol.* **1997**, *63* (1), 44−49.
(6) Makovitzki, A.; Avrahami, D.; Shai, Y. *Proc. Natl. Acad. Sci. U.S.A.* **2006**, *103* (43), 15997−16002.
(7) Kracht, M.; Rokos, H.; Ozel, M.; Kowall, M.; Pauli, G.; Vater, J. *J. Antibiot.* **1999**, *52* (7), 613−619.
(8) Sheppard, J. D.; Jumarie, C.; Cooper, D. G.; Laprade, R. *Biochim. Biophys. Acta* **1991**, *1064* (1), 13−23.
(9) Nicolas, J. P. *Biophys. J.* **2003**, *85* (3), 1377−1391.

surfactin into the lipid bilayers, causing permeability changes and/or membrane disruption.[12] Similar studies have been made of the interaction of other peptides with phospholipid bilayers.[13−15] A range of surfactin-lipid systems at surfaces have been studied by FT-IR,[16] AFM,[11] NMR,[12] and computer simulation.[9] These studies have concluded that surfactin can penetrate into a phospholipid monolayer at the air−water interface. However, the unsymmetrical nature of a monolayer is fundamentally different from that of a bilayer, and the driving forces for the interaction will be very different in the two cases. Apart from our paper using silica as a substrate,[2] Brasseur et al.[17] have used AFM to study the effect of incorporating surfactin into a DPPC bilayer supported on mica, where surfactin induced a ripple phase at concentrations (relative to DPPC) as low as 15%. The conditions of deposition in these experiments suggest that their experiment is far from equilibrium. Thus, their concentrations of DPPC and surfactin were both much higher than ours, and they used unilamellar vesicles created by sonication and filtration for their deposition. This does not invalidate their observations, but it makes it almost impossible to compare them with ours. At the conditions they used we would have expected no deposition of such a mixed bilayer on silica. Given that mica is much more negatively charged than silica, it is surprising that a mixed layer could have been formed on mica. The repulsion between mica and the mixture may be the reason for the occurrence of the ripple phase, which would only be attached lightly to the surface. In the present paper we are primarily concerned with the different issue of the mechanism of solubilization of the pure phospholipid bilayer by surfactin in solution. The same group has also shown that surfactin removes a mixed DOPC/DPPC bilayer from mica above the cmc, but no intermediate state between the presence and absence of phospholipid on the mica surface was observed and no information was obtained about the nature of the solubilized aggregate.[18] The aim of our experiments here is to access these missing details.

Experimental Methods

For the neutron reflectometry experiments, two of the silicon crystals were $125 \times 50 \times 25\ mm^3$ and one was $50 \times 60 \times 10\ mm^3$. They were polished on the large (111) face. The silicon substrate was cleaned by immersion in a 5:4:1 mixture of H_2O:H_2SO_4:H_2O_2 (piranha acid) at 85 °C for 15 min, followed by copious rinsing with clean water (UHQ, resistivity $>18\ M\Omega\ cm^{-1}$). Note that when preparing the piranha solution, the peroxide should always be added to the acid. The H_2O_2 is added immediately before the etching process because it reacts exothermically with a large release of gas. It was then treated in UV/ozone following a modification of the procedure first used by Brzoska.[19] Short wavelength UV was produced by a quartz mercury vapor lamp inside a glass tube, and the silicon crystal was placed inside the tube, through which oxygen flowed. The silicon was left in the UV/ozone for 30 min. This procedure removes any organic impurities and also improves the hydrophilicity of the surface.

The solution was held in a Teflon container (volume ~13 mL) and clamped against the silicon block between temperature-controlled aluminum and magnetic stirrer plates. The Teflon container had inlet and outlet ports located on opposite sides, which were connected to plastic tubes for injection of solution. Stirring of the solution was achieved by a magnetic flea placed in a compartment in the base of the trough and a small magnetic stirrer plate clamped behind the sample housing. Stirring was not however possible for the vertically held sample.

Three isotopic species of dipalmitoylphosphatidylcholine were used, designated h-DPPC (fully protonated), d_{31}-DPPC (one chain deuterated), and d_{75}-DPPC (fully deuterated). They were purchased from Avanti Polar Lipids and were stored at −20 °C. Surfactin is a naturally occurring cyclic lipopeptide produced from *Bacillus subtilis*. In our first paper we used protonated and deuterated samples prepared and analyzed by ourselves. Here, because the phospholipids are readily available in various deuterated forms, sufficient contrast variation could be obtained by using just the protonated form. This was purchased from Sigma-Aldrich (purity >98%) and was used without further purification. The sample was characterized by surface tension and found to be very similar in cmc and limiting surface tension to our own preparations, which had been fully characterized by mass spectrometry.[1]

The supported bilayer was formed by phospholipid (DPPC) coadsorption with β-D-dodecylmaltoside (DDM) from a molar ratio of 1:6 at concentrations of 0.141−0.123 g/dm^3 in D_2O or CmSi followed by further adsorption from 10 to 100 times more dilute solutions.[20,21] Each concentration was allowed to equilibrate for 1.5 h with the surface and then rinsed with 30 mL of water to remove DDM before injecting the next diluted concentration. After initial deposition of a mainly lipid layer, contact with the diluted solution leads to an exchange between surface and bulk aggregation which enriches the bilayer with insoluble lipid. This method has been shown to be capable of producing a dense bilayer after three steps of dilution when the DDM is also completely eliminated.

Two water contrasts were used, D_2O and CmSi (contrast matched to silica). CmSi was made by mixing high-purity H_2O (SLD = -0.57×10^{-6} Å^{-2}) and D_2O (SLD = 6.35×10^{-6} Å^{-2}) to give a scattering length density the same as silicon of 2.07×10^{-6} Å^{-2}. In the fitting of the data the scattering length densities of the phospholipids were calculated from volumes of the fragments estimated from molecular dynamics simulations.[22,23] These have been shown to be in good agreement with experimental data from density[24] and X-ray/neutron diffraction measurements.[25] Table 1 lists the scattering length densities of each DPPC used in the fitting of the neutron reflectivity data. The values calculated for surfactin were based on the known formula and estimated volumes of the fragments and the assumption that all the labile hydrogens of the amino acid residues can exchange with the solvent and are given in Table 2. Following the phospholipid deposition process phosphate buffered saline (PBS) buffer at pH 7.4 was used as the supporting solution.

The neutron reflection measurements were carried out on the SURF reflectometer at the ISIS pulsed neutron source at the Rutherford Appleton laboratory, UK,[26] and on the D17 reflectometer at the Institute Laue-Langevin in Grenoble, France.[27] All measurements were done in the time-of-flight mode, using a

(10) Deleu M., P. M. *C. R. Chim.* **2004**, *7*, 641–646.
(11) Deleu, M.; Nott, K.; Brasseur, R.; Jacques, P.; Thonart, P.; Dufrene, Y. F. *Biochim. Biophys. Acta* **2001**, *1513* (1), 55−62.
(12) Heerklotz, H.; Wieprecht, T.; Seelig, J. *J. Phys. Chem. B* **2004**, *108* (15), 4909−4915.
(13) Ringstad, L.; Schmidtchen, A.; Malmsten, M. *Langmuir* **2006**, *22* (11), 5042−5050.
(14) Ringstad, L.; Kacprzyk, L.; Schmidtchen, A.; Malmsten, M. *Biochim. Biophys. Acta* **2007**, *1768* (3), 715−727.
(15) Liu, X. H.; Huang, W. M.; Wang, E. K. *J. Electroanal. Chem.* **2005**, *577* (2), 349−354.
(16) Ferre, G.; Besson, F.; Buchet, R. *Spectrochim. Acta, Part A* **1997**, *53* (4), 623−635.
(17) Brasseur, R.; Braun, N.; El Kirat, K.; Deleu, M.; Mingeot-Leclercq, M. P.; Dufrene, Y. F. *Langmuir* **2007**, *23* (19), 9769−9772.
(18) Francius, G.; Dufour, S.; Deleu, M.; Papot, M.; Mingeot-Leclercq, M. P.; Dufrene, Y. F. *Biochim. Biophys. Acta* **2008**, *1778* (10), 2058−2068.
(19) Brzoska, J. B.; Shahidzadeh, N.; Rondelez, F. *Nature* **1992**, *360*, 719.
(20) Vacklin, H. P.; Tiberg, F.; Fragneto, G.; Thomas, R. K. *Langmuir* **2005**, *21* (7), 2827−2837.
(21) Tiberg, F.; Harwigsson, I.; Malmsten, M. *Eur. Biophys. J. Biophys. Lett.* **2000**, *29* (3), 196−203.
(22) Armen, R. S.; Uitto, O. D.; Feller, S. E. *Biophys. J.* **1998**, *75*, 734–744.
(23) Petrache, H. I.; Feller, S. E.; Nagle, J. F. *Biophys. J.* **1997**, *72*, 2237–2242.
(24) Costigan, S. C.; Booth, P. J.; Templer, R. H. *Biochim. Biophys. Acta* **2000**, *1468*, 41–54.
(25) Wienre, M. C.; White, S. H. *Biophys. J.* **1992**, *61*, 434–447.
(26) ISIS, World Wide Web page http://www.isis.rl.ac.uk/.
(27) ILL, World Wide Web page http://www.ill.fr.

Table 1. Scattering Length Densities of Different Contrasts of Dipalmitoylphosphatidylcholine (DPPC) and Surfactin in CmSi and D_2O

properties	hDPPC	d_{31}DPPC	d_{75}DPPC	surfactin (CmSi)	surfactin (D_2O)
$b/10^{-5}$ Å^{-1}	27.50	415.35	808.38	17.75	24.69
V/Å^3	1216	1216	1216	1516	1516
M/g mol^{-1}	734	764	810	1036	1045
$\rho/10^{-6}$ Å^{-2}	0.226	3.42	6.65	1.17	1.63
$b_{\text{headgroup}}/10^{-5}$ Å^{-1}	60.04	60.04	195.39	19.13	23.99
$V_{\text{headgroupg}}$/Å^3	326	326	326	1143	1143
$\rho_{\text{headgroupg}}/10^{-6}$ Å^{-2}	1.84	1.84	5.99	1.67	2.10
$b_{\text{chains}}/10^{-5}$ Å^{-1}	−32.54	355.30	612.98	−1.38	−1.38
V_{chains}/Å^3	889	889	889	373	373
$\rho_{\text{chains}}/10^{-6}$ Å^{-2}	−0.36	3.99	6.89	−0.37	−0.37

Table 2. Scattering Length Densities of Surfactin (in CmSi and D_2O)

properties	surfactin (CmSi)	surfactin (D_2O)
$b_{\text{total}}/10^{-5}$ Å^{-1}	17.75	24.69
M/g mol^{-1}	1036	1036
$\rho_{\text{total}}/10^{-6}$ Å^{-2}	1.17	1.63
$b_{\text{headgroup}}/10^{-5}$ Å^{-1}	19.1	24.0
$V_{\text{headgroupg}}$/Å^3	1143	1143
$\rho_{\text{headgroupg}}/10^{-6}$ Å^{-2}	1.67	2.10
$b_{\text{chains}}/10^{-5}$ Å^{-1}	−1.38	−1.38
V_{chains}/Å^3	373	373
$\rho_{\text{chains}}/10^{-6}$ Å^{-2}	−0.37	−0.37

wavelength, λ, range 0.5−6.6 Å on SURF and 2.2−19 Å on D17. All experiments were done at 298 K. The calibration of the reflectivity was made either by comparison with the totally reflected intensity below the critical angle with a solution in place that has a critical angle (SURF) or by direct scaling to the incident beam intensity (D17).

In a neutron reflectivity measurement the specular reflectivity R is measured as a function of Q (where Q is the wave-vector transfer normal to the surface or interface and defined as $Q = 4\pi \sin\theta/\lambda$, where θ is the grazing angle of incidence and λ is the neutron wavelength). The conventional method for calculating reflectivities uses the optical matrix method.[28] In this method the layer is divided into as many sublayers as is convenient or appropriate, and a characteristic matrix is evaluated for each sublayer, from which the whole reflectivity can be calculated exactly. It is then compared with the observed reflectivity, and the process is repeated until a satisfactory fit is obtained. Here, the reflectometry data were fitted using an interactive Java program based on the optical matrix method and adapted specially to the present system. The parameters of the oxide layer on silica were fixed as determined experimentally and the remaining layer divided into four adjustable layers, a possible surfactin layer on the outside away from silicon and then the heads, chains, and heads of the phospholipid bilayer. The adjustable parameters were the coverage of phospholipids and surfactin, the dimensions and penetration of surfactin into the bilayer, and the thicknesses of the four layers. All adjustments were subject to packing constraints using the volumes listed in Tables 1 and 2. The parameters were varied manually to obtain an optimum fit as judged by least-squares minimization on a log reflectivity plot.

The small-angle scattering experiments were done on the D11 small-angle neutron scattering instrument (SANS) at the Institut Laue Langevin, Grenoble.[27] The data were corrected for transmission and solvent background and converted to absolute intensity using standard procedures. The modeling was special to the present work and is discussed with the presentation of the data below.

Results: Neutron Reflectometry

Interaction of Surfactin with Supported Bilayers of h-DPPC. Before deposition of the supported bilayer, the Si−SiO_2 surface was characterized in both D_2O and CmSi to make sure that the thickness of native oxide layer and the surface roughness were all within an acceptable range. For the present samples, the fitted SiO_2 thickness was 15 ± 1 Å with a surface roughness of 3 Å. These values were used as the first layer in fitting the rest of the data. In our previous papers we have shown that surfactin has a compact ball-like structure with a diameter in the region of 13−15 Å,[1] which it seems to retain in the phospholipid bilayer.[2] The data obtained in the present experiment are not as sensitive to the structure and position of the surfactin, as our earlier data on the premixed bilayers so we constrained the surfactin dimensions to the values obtained in the earlier paper in all the fitting procedures.

The first stage of the experiment was the preparation of an h-DPPC layer from the mixed h-DPPC−DDM solution. Figure 1a shows the neutron reflectivity profiles of the mixed h-DPPC−DDM supported bilayers at three different stages of adsorption from D_2O (the profiles have been displaced by factors of 5, 25, and 125 for clarity of presentation). The reflectivity profiles were recorded after exposure for 11/2 h to each of the mixed h-DPPC−DDM solutions with intervening rinses by D_2O, except for the last rinsing where the solution was replaced by D_2O−PBS buffer at pH 7.4. The main changes occur between the first and second solutions, and the reflectivity profiles in Figure 1a show relatively little change after the second addition of solution to the cell.

The main difference in scattering length density is between the hydrophobic chains and hydrophilic headgroup regions of the h-DPPC bilayer because of the presence of D_2O in the latter. For the purposes of fitting the data the structure was therefore separated into three sublayers: the two headgroup regions and the central chain region. The overall phospholipid coverage (taken as the proportion of the surface occupied by the chain region of the bilayer) and bilayer thickness obtained from a single layer fit to the h-DPPC bilayer were taken as the starting point of the fitting. Three other adjustable parameters were then introduced: (i) the ratio of volume fraction of head 1 (next to the silica) to that of head 2, to allow for possible asymmetry in the headgroup distribution (if the ratio of head 1 to head 2 is set to 2, there are twice as many lipid molecules in the outer leaflet compared with the inner leaflet); (ii) the fraction of heads in the chain region, to allow for mixing disorder; and (iii) the interfacial roughness. In practice, these parameters, particularly (ii), allow for the presence of defective regions in the bilayer, which can be expected to increase as the amount of surfactin increases. The component volumes and scattering length densities needed in these calculations are given in Table 1. The various parameters were adjusted until a satisfactory fit was obtained. The results, given in Table 3, show that a bilayer with lower coverage was first formed by adsorption from the 0.141 g/dm^3 solution of 1:6 h-DPPC−DDM solution, and then the bilayer coverage gradually increased by about 10% as dilution proceeded. The thickness of the final bilayer in PBS buffer from the fitting was 56 ± 2 Å divided into

(28) Zhou, X. L.; Chen, S. H.; Felcher, G. P. *J. Phys. Chem.* **1991**, *95* (23), 9025−9029.

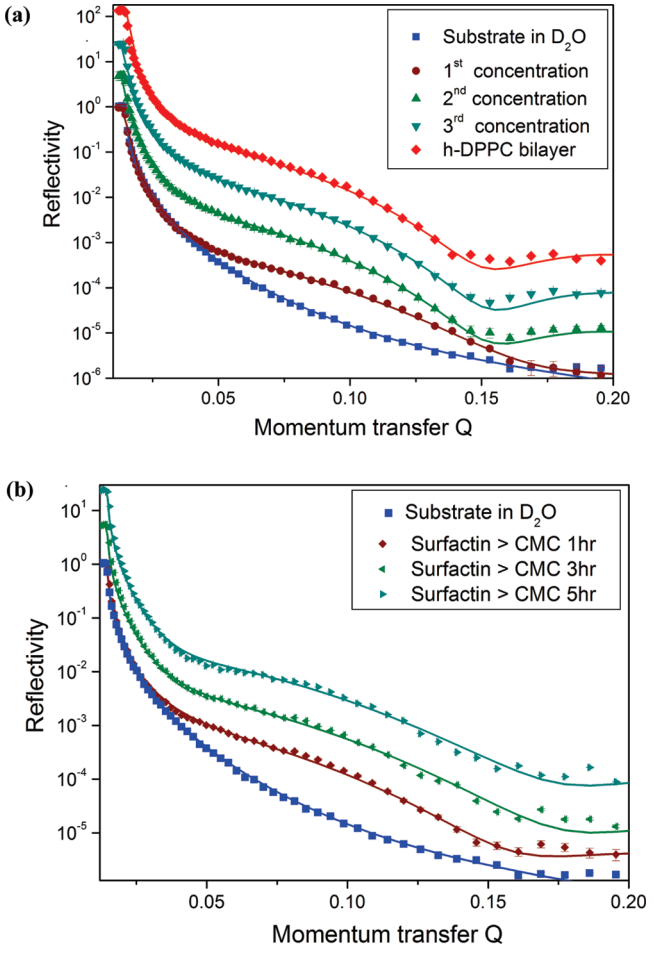

Figure 1. (a) Formation of h-DPPC bilayers via coadsorption with β-D-dodecylmaltoside. The top three profiles have been scaled up 5, 25, and 125 times for clarity. (b) Interaction of surfactin ([M] = 10^{-5} M) with h-DPPC bilayers in D_2O−PBS buffer at pH 7.5. The reflectivity profiles were recorded continuously after 1, 3, and 5 h and are scaled up for 5 and 25 times for clarity.

2 × 8 and 40 Å respectively for head and chain sublayers. The phospholipid coverage was 0.90 ± 0.02. All the results from the bilayer, including the intermediate stages, are in reasonable agreement with results from other experiments on supported DPPC bilayers. Vacklin et al.[20] also showed, using mixtures of DPPC and d_{25}-DDM mixtures, that all of the DDM surfactant is exchanged with phospholipid during the first rinsing and adsorption step, after which only minor changes occur in the bilayer structure. From the similarity of the two sets of results it is reasonable to conclude that the same is true for the present bilayers.

Following the establishment and characterization of the h-DPPC bilayer, the solubilization of the supported h-DPPC by surfactin in the external solution was investigated. The interaction of surfactin with the bilayer was divided into two steps: one below and one above the cmc (5 × 10^{-6} M). At 10^{-6} M surfactin in D_2O−PBS buffer at pH 7.5, the total intensity of the reflectivity profile did not change dramatically with time, but it shows a slightly steeper decline with Q than the complete DPPC bilayer (Figure 1b). Since a steeper decline is always associated with a thicker layer this suggests, without any quantitative analysis, that there is some adsorption of surfactin in or on the outer part of the bilayer. When the surfactin concentration is increased above the cmc to 10^{-5} M, the reflectivity changes substantially, and it is clear that there is now also a significant removal of bilayer material at this concentration. The fitted parameters at the different stages of the surfactin addition are listed in Table 4.

At this isotopic composition the reflectivity is sensitive to both phospholipid and surfactin coverages but less sensitive to the position of the surfactin. A reasonable fit to the low surfactin concentration data could be obtained with no penetration of surfactin into the h-DPPC bilayer, but the fit improved if the surfactin molecules were partially embedded in the outer part of the DPPC bilayer forming a sublayer of thickness of 15−20 Å. This is consistent with the more definitive location of surfactin in the bilayer reported in our previous paper.[2] At the low concentration of surfactin the bilayer remains more or less unchanged but with a small amount of surfactin at a volume fraction of 0.08 ± 0.03 and a penetration 15 ± 5 Å with the surfactin lying close to the headgroup region. When the concentration of surfactin is above the cmc, the neutron reflectivity profiles change significantly in the first hour, and the fitted data in Table 4 show that the phospholipid coverage was significantly reduced from 0.89 to 0.52 over the space of 5 h while the surfactin coverage increased from 0.08 to 0.26. Again surfactin was found to penetrate 15−20 Å into the outer chain region.

Surfactin Interaction with a d_{31}-DPPC Bilayer. The native oxide surface was again first characterized in both D_2O and CmSi to give an oxide layer thickness of about 14 Å and a surface roughness of 5 Å (different solid sample). The neutron reflectivity profiles in Figure 2a show the blank surface in D_2O and CmSi and the formation of a d_{31}-DPPC−DDM supported bilayer following the procedure described above from three different adsorption stages with intervening rinses with D_2O. The fringe in the d_{31}-DPPC bilayer is different from that for h-DPPC and is now below the D_2O profile, whereas in the h-DPPC it was above the D_2O (compare the initial profiles in Figures 2a,b). The reason is that the scattering is now only from one lipid chain and the headgroup and thus the contrast with D_2O is lower. Although the d_{31}-DPPC makes a smaller contribution to the reflectivity, it has sufficient contrast with the D_2O to define the bilayer coverage, but it has a different sensitivity to changes in the bilayer.

Figure 2b presents the effects of solubilization of the d_{31}-DPPC bilayer by 10^{-6} and 10^{-5} M surfactin. There is a small change with the lower concentration, but there is a dramatic drop of the fringe of the d_{31}-DPPC bilayer when the surfactin concentration is above its cmc. In the first hour, the fringe is lower than for the bilayer, and then it disappears after 6 h and the reflectivity moves toward that of D_2O. There is a further shift toward the D_2O profile over 12 h, but the reflectivity finally reaches a stable value showing that the surfactin does not remove the bilayer completely.

The fitted results for the d_{31}-DPPC bilayer and surfactin interaction with d_{31}-DPPC bilayers are summarized in Table 5. The final d_{31}-DPPC bilayer shows a fairly high coverage of about 0.84, although it shows a higher disorder with respect to mixing of chains and head groups than the h-DPPC. Approximately 9% of the bilayer is removed in the first 2 h. The strong bilayer fringe in the momentum transfer range of 0.04−0.1 $Å^{-1}$ disappears after 6 h of exposure to surfactin and the phospholipid coverage drops to 0.21, corresponding to a removal of 72% of the original bilayer, a much higher depletion than observed for the h-DPPC above. Solubilization continued for a further 2 h until the fitted phospholipid coverage reached 0.11. In the end the whole solubilization process became very slow, and the profile approached that of D_2O in 12 h but then remained constant (to 16 h). The surfactin coverage remained constant at around 0.15 instead of increasing as was observed for h-DPPC. In the h-DPPC bilayer the surfactin coverage increased up to 0.26 in 5 h, but the phospholipid

Table 3. Fitted Parameters and Calculated Properties of a Supported h-DPPC−DDM Bilayer on a Silica on Silicon Surface at Different Solution Concentrations

properties	0.14 g/dm^3	0.014 g/dm^3	0.0014 g/dm^3	bilayer
head 1 thickness/Å	6.5 ± 1	7.75 ± 1	8 ± 1	8 ± 1
chain thickness/Å	32 ± 1	36 ± 1	39.5 ± 1	40 ± 1
head 2 thickness/Å	7.5 ± 1	7.75 ± 1	8 ± 1	8.25 ± 1
phospholipid coverage	0.83 ± 0.02	0.86 ± 0.02	0.89 ± 0.02	0.90 ± 0.02
ratio head 1 to 2	1.2 ± 0.3	1.8 ± 0.5	1.8 ± 0.5	1.8 ± 0.5
fraction heads in chain	0.07 ± 0.02	0.08 ± 0.02	0.04 ± 0.02	0.06 ± 0.02
interfacial roughness/Å	6 ± 1	5.5 ± 1	6 ± 1	6 ± 1

Table 4. Fitted Parameters and Calculated Properties of Surfactin Interacting with h-DPPC Bilayers at 25 °C and Different Concentrations and Times

properties	bilayer	10^{-6}	10^{-5}, 1 h	10^{-5}, 3 h	10^{-5}, 5 h
head 1 thickness/Å	8 ± 1	8 ± 1	7.5 ± 1	7.5 ± 1	7 ± 1
chain thickness/Å	42 ± 1	41.5 ± 1	37.5 ± 1	37.5 ± 1	37.5 ± 1
head 2 thickness/Å	8 ± 1	8 ± 1	7.5 ± 1	7.5 ± 1	7 ± 1
phospholipid coverage	0.90 ± 0.02	0.89 ± 0.02	0.73 ± 0.02	0.63 ± 0.02	0.52 ± 0.02
fraction head 1 to 2	1.7 ± 0.5	4.0 ± 1.0	5.7 ± 1.0	4.6 ± 1.0	4.6 ± 1.0
fraction heads in chain	0.10 ± 0.02	0.10 ± 0.02	0.11 ± 0.02	0.09 ± 0.02	0.57 ± 0.02
surfactin thickness/Å	0	15	20	20	20
surfactin penetration/Å	0	8 ± 1	19 ± 1	21.5 ± 1	21 ± 1
surfactin coverage	0	0.08 ± 0.03	0.13 ± 0.03	0.26 ± 0.05	0.26 ± 0.05
interfacial roughness/Å	6 ± 1	6 ± 1	3.5 ± 1	3.7 ± 1	4.1 ± 1

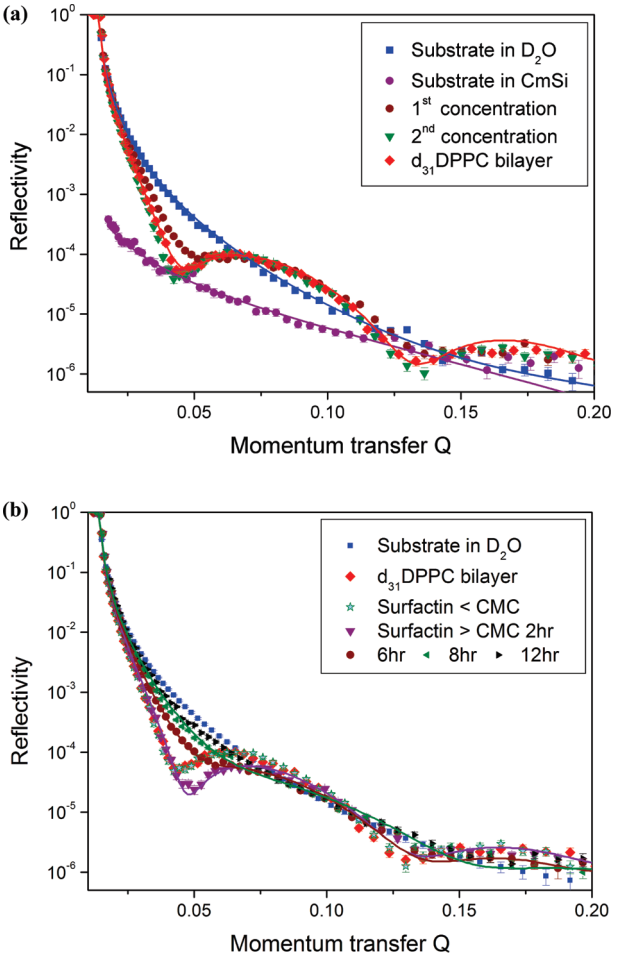

Figure 2. Neutron reflectivity profiles of (a) the formation of the d_{31}-DPPC bilayer via coadsorption with DDM in D_2O/PBS buffer at pH 7.5 and (b) interaction of surfactin at concentration of 10^{-5} M with d_{31}-DPPC bilayers.

coverage remained high (0.52). Since surfactin does not adsorb on its own on the silica surface,[1] it can only be present because of its attractive interaction with DPPC. It is then not surprising that the surfactin coverage is linked to the lipid coverage. The contrast between phospholipid and surfactin in this experiment is more sensitive to the location of the surfactin than for h-DPPC. This is related to the neutron reflectivity fringe falling below the D_2O profile rather than remaining above it.

Table 5. Fitted Results for Interaction of Surfactin with d_{31}-DPPC Bilayers at a Surfactin Concentration of 10^{-5} M

properties	bilayers	2 h	6 h	8 h
head 1 thickness/Å	8.5 ± 1	7 ± 1	6.25 ± 1	6.5 ± 1
chain thickness/Å	50 ± 1	45 ± 1	38 ± 1	34 ± 1
head 2 thickness/Å	8.5 ± 1	7.5 ± 1	6.5 ± 1	7.5 ± 1
phospholipid coverage	0.84 ± 0.02	0.76 ± 0.02	0.21 ± 0.02	0.11 ± 0.02
fraction head 1 to 2	2.0 ± 0.5	2.2 ± 0.5	7.3 ± 2.0	4.9 ± 2.0
fraction heads in chain	0.15 ± 0.1	0.10 ± 0.1	0.06 ± 0.1	0.15 ± 0.1
surfactin thickness/Å	0	11	21	21
surfactin penetration/Å	0	12.5 ± 1	19 ± 1	21 ± 1
surfactin coverage	0	0.34 ± 0.03	0.17 ± 0.03	0.10 ± 0.03
interfacial roughness/Å	4.5 ± 1	5.2 ± 1	5.4 ± 1	4.5 ± 1

Surfactin Interaction with the d_{75}-DPPC Bilayer. The d_{75}-DPPC experiment was similar to those described above but with a smaller cell volume and the smaller silicon block. The experiment was performed at ILL on D17 with the sample, and hence the surface, now in a vertical position. Again, the first step was to characterize the Si−SiO_2 surface in both D_2O and CmSi leading to a thickness of SiO_2 of about 16 Å and a surface roughness of 5 Å. The neutron reflectivity profiles during the three adsorption steps of d_{75}-DPPC and DDM in CmSi water are shown in Figure 3a.

The fitted results for the final bilayer are listed in Table 6. The reflectivity is again found to be sensitive to phospholipid coverage, and the final coverage of the d_{75}-DPPC bilayer was found to be 0.55 ± 0.02 with thicknesses of 8 and 37 ± 1 Å for the head and chain regions, respectively. The d_{75}-DPPC bilayers were less complete than the h-DPPC (0.9) and d_{31}-DPPC (0.84) bilayers. A probable reason for this low coverage is that it was not possible to incorporate a stirrer in the cell on D17 because of the vertical alignment of the block. The previous two systems were investigated in horizontal stirred cells. We have since found that stirring is an important factor in optimizing the deposition process.

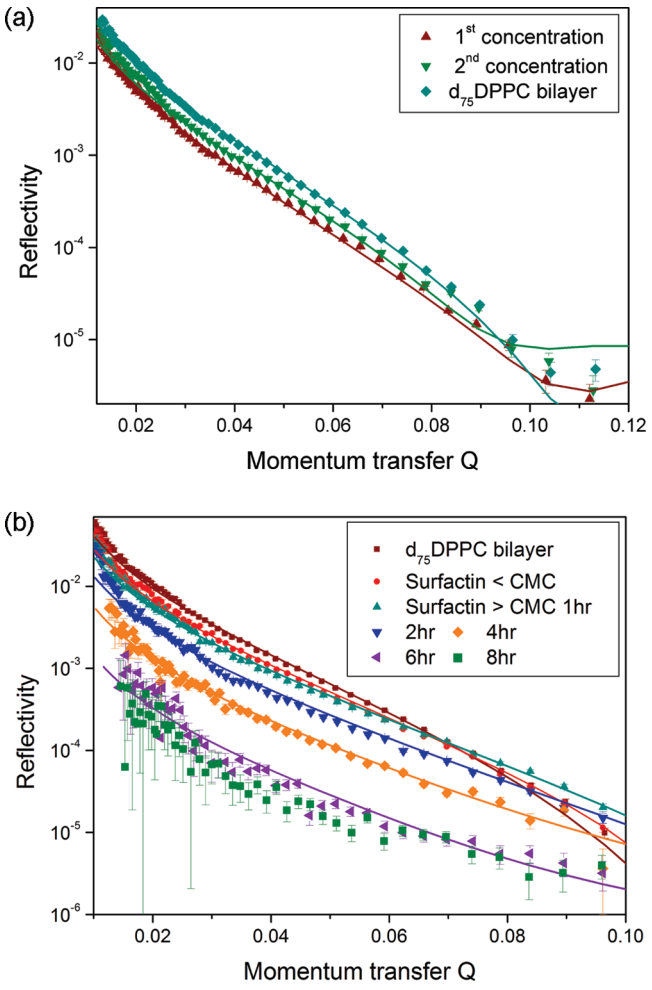

Figure 3. (a) Formation of d_{75}-DPPC supported bilayers via coadsorption with β-D-dodecylmaltoside at 25 °C in CmSi. (b) Interaction of surfactin with d_{75}-DPPC supported bilayers in CmSi−PBS buffer at 25 °C.

Table 6. Fitted Parameters and Calculated Properties of d_{75}-DPPC−DDM Supported Bilayers during Their Deposition on Silica

properties	0.14 g/dm^3	0.014 g/dm^3	bilayer
head 1 thickness/Å	8.25 ± 1	8.25 ± 1	8.25 ± 1
chain thickness/Å	34 ± 1	35.5 ± 1	37 ± 1
head 2 thickness/Å	8 ± 1	8 ± 1	8 ± 1
phospholipid coverage	0.41 ± 0.02	0.53 ± 0.02	0.57 ± 0.02
fraction head 1 to 2	1.0 ± 0.3	1.0 ± 0.3	1.0 ± 0.3
fraction heads in chain	0.37 ± 0.05	0.17 ± 0.05	0.14 ± 0.05
interfacial roughness/Å	4 ± 1	5 ± 1	4 ± 1

Surfactin was again injected into the cell as described above. The reflectivity profiles are shown in Figure 3, and the fitted results are shown in Table 7. These profiles were again found to be sensitive to phospholipid and surfactin coverage but less so to the other structural parameters. The surfactin penetration was therefore initially fixed at 15 Å, taken from the previous h-DPPC and d_{31}-DPPC results. The injection of surfactin concentration below the cmc caused a decrease of the d_{75}-DPPC reflectivity, suggesting the incorporation of surfactin with its now relatively much lower scattering length density into the d_{75}-DPPC bilayer. As expected, there is a sharp change when the surfactin concentration is increased to 10^{-5} M, and the coverage of the original d_{75}-DPPC decreased more rapidly than the other two bilayers, with the whole disappearing in 8 h. The reflectivity profiles had almost dropped to that of the bare surface in CmSi after 8 h of measurement.

Results: Small-Angle Neutron Scattering

To try to obtain a more complete understanding of the whole process of solubilization, it is necessary to know how the surfactin solubilizes the phospholipid in the bulk solution. SANS measurements were therefore performed over exactly the same range of concentration as the neutron reflection experiments. Mixtures were made up at a fixed h-DPPC concentration of 2 mM with different concentrations of surfactin (0.05, 0.1, 0.2, 0.4, and 0.6 mM) (0.4 mM corresponds to the approximate threshold concentration for solubilization of the supported bilayer). D_2O was used as solvent to give a good scattering contrast between solvent and the lipid−surfactin aggregates. Figure 4 shows the SANS profiles of the five mixed DPPC/surfactin ratios at 25 °C. The profile of the 2 mM DPPC/0.05 mM surfactin mixture shows a sharp Bragg peak at 0.11 Å^{-1}, which corresponds to a stack of DPPC bilayers probably in a multilamellar vesicle. The Bragg peak position at Q_p = 0.11 Å^{-1} gives a bilayer spacing, $d = 2\pi/Q_p$, of the DPPC multilamellar vesicles of 58 Å. With increasing surfactin concentration from 0.05 to 2 mM, the Bragg peak around 0.11 Å^{-1} remains at the same position, but an additional correlation peak starts to appear at lower Q (same parameter as in the reflection experiments), which moves to higher Q before finishing at around 0.04 Å^{-1}. For all solutions the slope of the plot at low Q (−2) indicates lamellar structures in the solution, and since there is no indication of any surfactin micelles, the surfactin must be dissolved in the DPPC bilayers. On its own surfactin forms small but well-defined micelles with an aggregation number of 20.[1] The presence of the correlation peak, which corresponds to a distance of about 150 Å, would require an approximate local concentration of surfactin (in the form of micelles) of 20 mM, a factor of 100 times the actual average concentration in the bulk. The only realistic way this could occur is if the surfactin aggregates are concentrated in the DPPC multilamellar vesicles. Taking the aggregation number of 20 for surfactin from the earlier SANS data and an volume per aggregate of $4\pi \times 25^3/3$ Å^3 gives a molar ratio of surfactin to DPPC of about 0.1 in the vesicles at the highest surfactin concentration. This would be all of the surfactin at the middle concentration used (0.2 mM surfactin), and hence all of the surfactin must be concentrated in the phospholipid lamellar structures rather than some of it occurring as free micelles. Since the lamellae in the vesicle are about 58 Å apart most of which is phospholipid, not water, the most probable location of the surfactin aggregates is straddling the bilayers as pores or micelles. The attractive interaction between surfactin and the DPPC could be sufficient to account for the stabilization of the DPPC vesicles.

There are no models in the literature for treating the scattering from such structures at present. However, we have adopted the approximate procedure of subtracting the lowest concentration profile (purple dashed line) from the high concentration profile (green dashed line) to produce the data in Figure 5. The subtraction removes the Bragg peak at Q of around 0.11 Å^{-1} and leaves the contributions from the correlation peaks at around 0.04 Å^{-1}. The fits of a standard core−shell model for the surfactin aggregates using the same fragment volumes as for the reflectivity and an adjustable effective concentration, as though the solution were a uniform micellar solution, gives the calculated line in Figure 7. Considering the approximate nature of the calculation the fit is remarkably good and suggests that the aggregation number remains small at 50 ± 10 with a total radius of 27 ± 4 Å. The separation of the surfactin aggregates in the multilamellar vesicle is found to be about 160 Å. While the precision of these parameters is not high and a range of aggregate structures might

Table 7. Fitted Parameters and Calculated Properties of Surfactin Interaction with d_{75}-DPPC Bilayers at Different Surfactin Concentrations and Times

properties	10^{-6}	10^{-5}, 1 h	10^{-5}, 2 h	10^{-5}, 4 h
head 1 thickness/Å	8.25 ± 1	7.5 ± 1	7 ± 1	7 ± 1
chain thickness/Å	37 ± 1	36 ± 1	36 ± 1	33 ± 1
head 2 thickness/Å	8 ± 1	7 ± 1	7 ± 1	7 ± 1
phospholipids coverage	0.53 ± 0.02	0.49 ± 0.02	0.46 ± 0.02	0.28 ± 0.02
fraction head 1 to 2	1.8 ± 0.5	2.1 ± 0.5	1.6 ± 0.5	1.6 ± 0.5
fraction heads in chain	0.04 ± 0.03	0.04 ± 0.03	0.04 ± 0.03	0.04 ± 0.03
surfactin thickness/Å	13.25	13	15	15
surfactin penetration/Å	10.5 ± 1	10.5 ± 1	18 ± 1	15 ± 1
surfactin coverage	0.15 ± 0.03	0.22 ± 0.03	0.36 ± 0.05	0.32 ± 0.05
interfacial roughness/Å	4.5 ± 1	4.5 ± 1	4.8 ± 1	4.0 ± 1

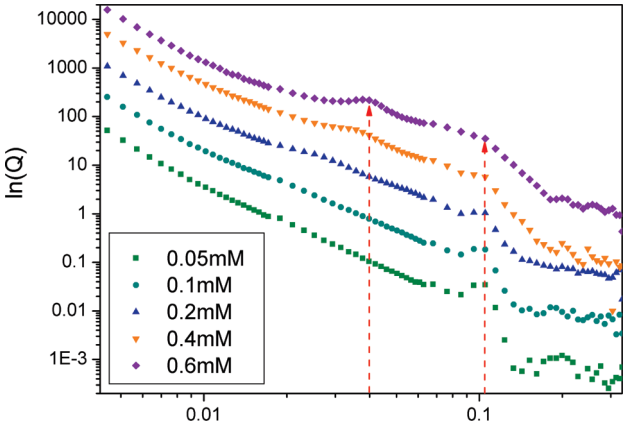

Figure 4. SANS profiles measured for DPPC/surfactin mixtures in D_2O. The arrows indicate the corresponding Bragg peaks for each phase. The graphs are scaled for clarity.

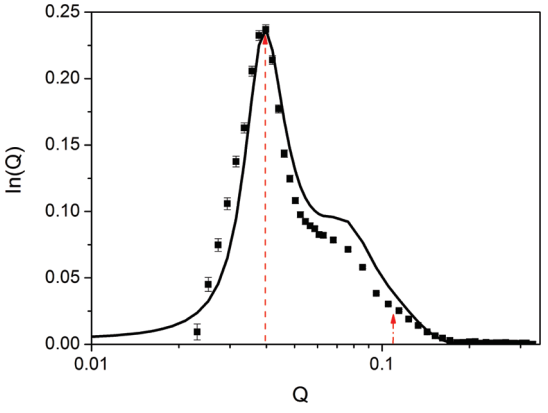

Figure 5. Small-angle neutron scattering fit (solid lines) using a core−shell model and an effective local concentration to fit the position of the correlation peak (160 Å) for the scattering profile for 2 mM DPPC + 0.6 mM surfactin less that of 2 mM DPPC + 0.05 mM surfactin.

also be fitted to the data, the basic result is that, above its cmc, surfactin forms aggregates of an aggregation number of about 50 in the DPPC bilayer structure. The dimensions, as assessed from the aggregation number, suggest that the aggregates are of a size to span the bilayer. The aggregates would have to be quite different from the micelles that exist in aqueous solution because of the different environment but the data do not warrant more precise modeling.

Recently Kell et al.[29] published SANS and TEM results for surfactin/DMPC mixtures, in which they concluded that vesicles predominate at surfactin concentrations less than 4 mol %, but bilayer membrane fragments started forming when the surfactin concentration was increased. Up to 15 mol % surfactin concentration, small DMPC−surfactin micelles of ellipsoidal conformation were found. For DPPC/surfactin mixtures vesicle structures were retained up to concentrations of 30 mol % surfactin. The last result is consistent with our observations here.

The only system we have been able to find in the literature that shows similar scattering features to those observed here is for a dispersion of fullerenes (C_{60}) in phospholipid bilayers. C_{60} is hydrophobic and thus has a strong tendency to self-aggregate, and the scattering patterns do indeed show correlation peaks in the SANS consistent with C_{60} embedded in the DPPC bilayer.[30] That this occurs for an extremely hydrophobic molecule further reinforces the idea that surfactin is more like a mainly hydrophobic ball than a conventional surfactant.

Discussion

The neutron reflectometry results on the three different contrasts of DPPC−DDM supported bilayers are consistent with earlier results of Vacklin,[20,31] and the coverages of two of the three final DPPC bilayers are in the expected range for the supported bilayer, though lack of stirring reduced the bilayer coverage for the last experiment. Vacklin has, however, shown that bilayer coverages over 0.5 still function well as bilayers for studying the attack of the bilayer by the hydrolyzing enzyme, phospholipase (PLA_2).

The clearest results of the present work are that surfactin must be above its cmc for removal of the supported bilayer, i.e., surfactin must act by solubilizing the phospholipids, and that surfactin must interact attractively with DPPC, since it otherwise would not adsorb at all into the layer. The latter confirms the conclusion from our earlier paper and also the results obtained in bulk solution using isothermal calorimetry by Razafindralambo et al.[32] The results from our earlier paper suggested that the surfactin concentration can reach a threshold level of about 20 mol %. This was the maximum attainable concentration in the premixed bilayer, and this is likely to be close to the threshold for desorption of the mixture. The presence of a threshold is also supported by the slow initial removal of phospholipids from the surface. Figure 6 shows the decrease in phospholipid coverage of the three bilayers with time. For the two most complete initial bilayers, the phospholipid coverages initially decreased slowly in the first 2 h, generally by an amount less than 10%, before being removed more rapidly. The more rapid removal of the less

(29) Kell, H.; Holzwarth, J. F.; Boettcher, C.; Heenan, R. K.; Vater, J. *Biophys. Chem.* **2007**, *128* (2−3), 114−124.

(30) Jeng, U. S.; Hsu, C. H.; Lin, T. L.; Wu, C. M.; Chen, H. L.; Tai, L. A.; Hwang, K. C. *Physica B* **2005**, *357* (1−2), 193−198.

(31) Vacklin, H. P.; Tiberg, F.; Thomas, R. K. *Biophys. J.* **2003**, *84* (2), 177a−178a.

(32) Razafindralambo, H.; Dufour, S.; Paquot, M.; Deleu, M. *J. Therm. Anal. Calorim.* **2009**, *95* (3), 817−821.

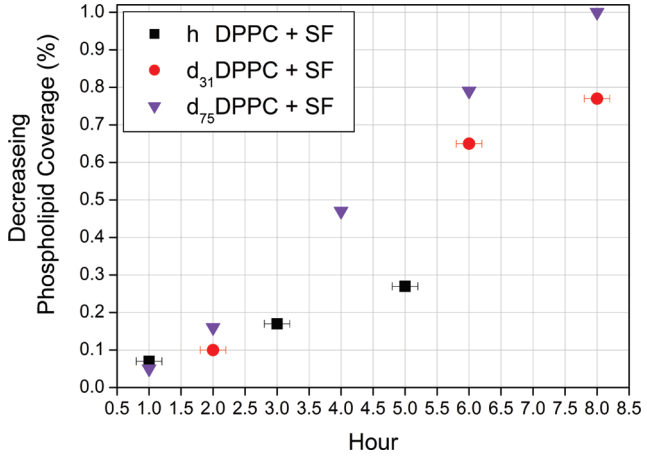

Figure 6. Comparison of decreasing phospholipid coverage (percentage) as a function of time.

complete layer may indicate that the initial accumulation of surfactin in this layer is much easier simply because there are more vacant sites (defects) for adsorption to occur. That this is probably the reason is also suggested by the rate of solubilization being inversely related to lipid coverage in the order h-DPPC, d_{31}-DPPC, and d_{75}-DPPC.

The slowest solubilization occurred for h-DPPC, which started with a high coverage of 0.9 and was still at a coverage of 0.64 after 5 h. For all of the reflectivity profiles recorded during this period the surfactin/phospholipid ratio is less than the 20 mol % estimated to be the approximate threshold for solubilization. For the other two bilayers the surfactin concentration is at or above the threshold for most of the measurements, and removal of the bilayer is faster and more complete. The difference in the amount of surfactin adsorbed into the bilayer suggests that defects are important. There should be many more of these in the two lower coverage bilayers. The extent of adsorption will be determined by the strength of the attractive interaction and the availability of space on the surface. Solubilization then seems to depend on four factors. First the bulk phase must contain micelles for removal of the bilayer to occur to any significant extent; i.e., it must be above the cmc. Second, the proportion of surfactant to DPPC must reach a threshold level in the bilayer. Third, there must be space for rearrangement into soluble aggregates within the supported bilayer, and this may be blocked when there is too much material on the surface, either phospholipid or too much phospholipid + surfactin. However, the one unexpected result is the failure of the process to go to completion for the d_{31}-DPPC and h-DPPC bilayers.

Figure 7 shows the distribution profiles of each component generated from the neutron results according to Table 4. By whatever means the surfactin eventually solubilizes the layer, the SANS experiments show that it involves the formation of surfactin aggregates, which would require substantial rearrangement in the layer from that shown in Figure 7c. However, even in the more sensitive conditions used in our previous paper,[2] no distribution of surfactin along the surface normal is observed that could be attributed to micelles or pores spanning the bilayer. However, it is important to note that neutron reflectometry does not distinguish any lateral inhomogeneity and, although the surfactin is in the outer layer, it is not necessarily uniformly in the plane of this layer. Even if there were clusters of surfactin in the outer half of the layer, considerable rearrangement would still be required to form an aggregate soluble in the bulk solution; i.e., the rearrangement of the surfactin to form micelles/pores in the

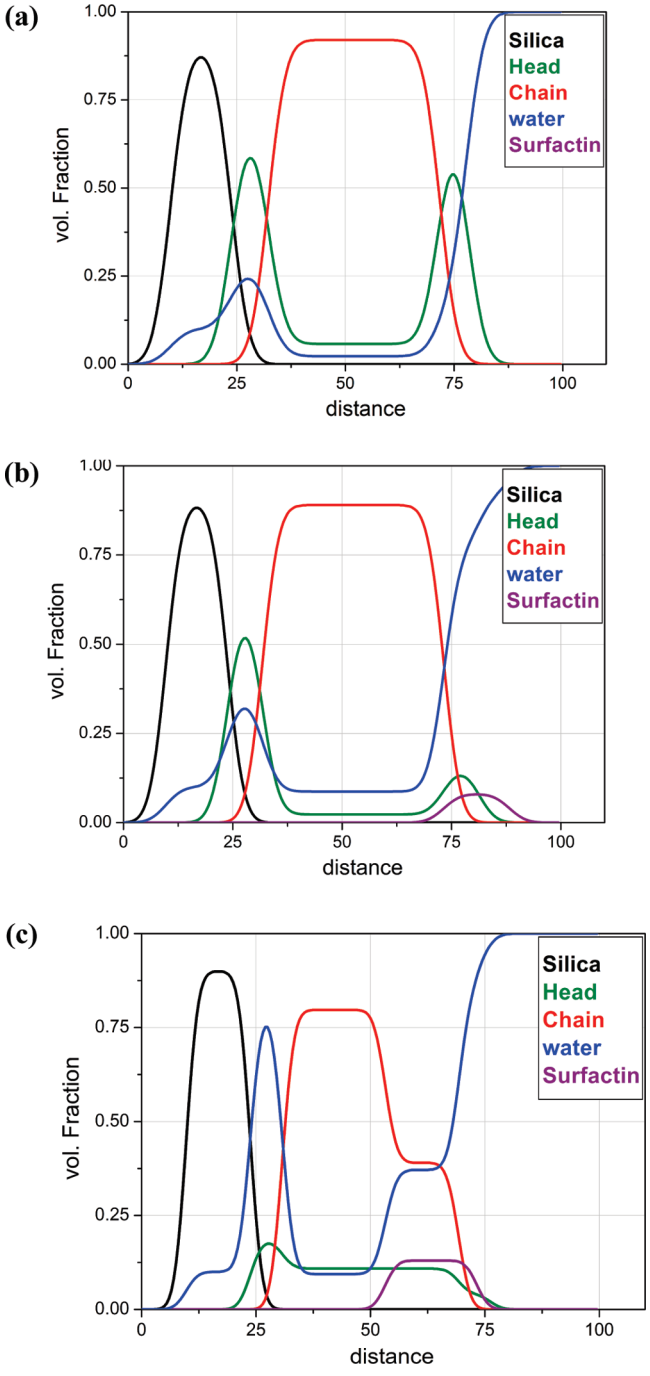

Figure 7. Distribution profiles of DPPC bilayers−surfactin interaction: (a) h-DPPC bilayer; (b) surfactin penetration into the h-DPPC bilayer; (c) solubilization effects after 5 h of exposure to surfactin ($M = 10^{-5}$).

supported bilayer is likely to be slow. At the pH of these experiments (pH 7.4) the surfactin would carry a double negative charge in solution as the monomer. As discussed previously, this is the probable reason why surfactin resides in the outer layer of the leaflet, silica being weakly negatively charged, even though the surfactin might not be as completely ionized in the bilayer. As surfactin rearranges to form aggregates there will come a point where the accumulated negative charge causes rapid desorption because of the electrostatic repulsion between surfactin and silica. Such a process could account for such structures not being observed.

As discussed in the Introduction, Francius et al.[18] have also observed the removal of supported phospholipid bilayer on mica

by surfactin using AFM. Our results show some of stages of this process, in particular the incorporation of surfactin into the outer region of the bilayer, a threshold concentration of surfactin, and the final surfactin aggregates in the solubilized vesicles. The much higher negative charge on mica compared with silica would make the first two processes much harder to see on mica. Our results give some experimental substance to the results proposed from computer simulation by Deleu et al.[33]

Conclusions

Supported DPPC membranes are progressively removed from the surface by surfactin in the solution above its cmc (5×10^{-5} M) but not below. The first action of surfactin is to penetrate into the outer leaflet of the membrane bilayer until it reaches a threshold concentration. This process only proceeds further if the surfactin is above its cmc, when the phospholipids are then progressively removed. At the same concentration, the structure of the solution shows that surfactin forms micelles or pores in the DPPC vesicles, indicating that the process of desorption involves rearrangement of the surfactin in the supported bilayer. Such a rearrangement is expected to be slow, which may explain why mixtures of surfactin and DPPC above the cmc of surfactin do not adsorb on a silica surface[2] and why the desorption is also slow. While it may not be possible to generalize this pattern of behavior to other phospholipids, the mode of action of surfactin in these experiments may be a major factor in the origin of its antibiotic and other biological effects.

Acknowledgment. H.H.S. thanks the Swire foundation for a scholarship. We thank STFC and the Institut Laue-Langevin for the provision of neutron scattering facilities at ISIS and ILL.

Supporting Information Available: Chemical structure of surfactin. This material is available free of charge via the Internet at http://pubs.acs.org.

(33) Deleu, M.; Bouffioux, O.; Razafindralambo, H.; Paquot, M.; Hbid, C.; Thonart, P.; Jacques, P.; Brasseur, R. *Langmuir* **2003**, *19* (8), 3377−3385.